

Design of 2.45GHz Circularly Polarized Tag Antenna

Chung-Long Pan¹, Shuming T. Wang¹, Ping-Cheng Chen^{2,*}, and Yen-Fu Chen¹

¹ Department of Electrical Engineering, I-Shou University, Kaohsiung City, Taiwan;
Email: ptl@isu.edu.tw (C. L.P.), smwang@isu.edu.tw (S. T.W.), caker123789@gmail.com (Y. F.C.)

² Department of Intelligent Network Technology, I-Shou University, Kaohsiung City, Taiwan;
Email: chen1113@isu.edu.tw (P.C.C.)

*Correspondence: chen1113@isu.edu.tw (C.L.P.)

Abstract—This paper presents the design and development of a circularly polarized (CP) tag antenna to overcome the polarization mismatch between the reader antenna and the tag antenna in RFID systems. This CP antenna is designed at 2.4 GHz for radio frequency identification (RFID) applications. It consists of a simple square loop loaded with an open gap, two feeding strips, and a matching stub. The antenna is fabricated on an FR4 substrate with a dielectric constant of 4.4, a dielectric loss tangent of 0.02, and a thickness of 0.8mm. In order to achieve conjugate matching between the circular tag antenna and the tag chip, the technique of loading a matching short line on the tag chip was used. Additionally, the radiation of circular polarization (CP) was achieved by placing an open gap and two feeding strips on the square loop. Through electromagnetic simulation analysis, the antenna performance is evaluated. The reflection coefficient (S11) at 2.45 GHz is measured to be -17.16^{dB} , indicating good impedance matching. The 3 dB axial ratio bandwidth is 0.19 GHz (7.7%), covering the frequency range of 2.34 GHz to 2.53 GHz. The 10th power reflection bandwidth is approximately 8.9% (2.33 GHz to 2.55 GHz), ensuring broad operational bandwidth. The antenna also exhibits a favorable antenna gain of 2.29^{dBi} . This study successfully demonstrates the design and performance evaluation of a CP tag antenna for RFID applications

Keywords—RFID, tag antenna, circularly polarized

I. INTRODUCTION

Radio frequency identification (RFID) has been considered as an important key technology that affects global business logistics management systems and warehouse management systems. In addition to traditional applications, there is an increasing interest in using RFID technology for surveillance purposes. By deploying RFID sensors strategically, it is possible to track the movement of individuals and objects within defined areas. This has significant applications in security systems, access control, and even ensuring personal safety in environments such as hospitals or hazardous areas. By integrating RFID tags with sensors that measure parameters like temperature, humidity, air quality, and water quality, real-time data can be collected from different locations. This data can be

utilized for monitoring and managing environmental conditions, detecting anomalies, and making informed decisions regarding environmental protection, disaster management, and pollution control. The combination of RFID with wireless sensor networks (WSNs) and unmanned aerial vehicles (UAVs) can be employed for various applications such as large-scale surveillance, aerial surveys, and real-time data collection. All of frequency ranges for RFID applications can be classified as follows [1].

Low frequency (LF) band: (9-135 kHz)

High frequency (HF) band: (13.56, 27.125, 40.68 MHz)

Ultra-high frequency (UHF) band:(433.9, 869, 915 MHz)

Microwave band: (2.45, 5.8, 24.125 GHz)

Most of the UHF/Microwave RFID tag antennas designed using linearly polarized methods, like dipole antennas, microstrip antennas, and inverted F antennas. But in some RFID applications, such as vehicle access management systems, the need for long-distance communication capabilities is necessary. In order to increase the reading distance of the RFID system, the use of active tags can achieve this purpose, but the production cost of such tags is higher. It is known from the literature that the use of circularly polarized (CP) antennas reduces the sensitivity of wireless communication systems to antenna orientation than linearly polarized antennas. When the tag antenna also uses an antenna with circular polarization radiation, and the reader and the tag antenna are matched, it can increase the reading distance effectively.

Among the traditional circularly polarized antennas, microstrip, spiral, waveguide and loop antennas were all widely used [2–5]. In [4], a circularly polarized tag antenna was designed with a microstrip antenna. Its antenna area (189 mm × 127 mm) and thickness (21.6 mm) are very large, which is not suitable for practical applications. In [5], basically, two dipoles and matching circuits were used to achieve the circular polarization function. To achieve miniaturization, for ease of manufacturing and, loop antennas are more suitable for

RFID applications than microstrip antennas that require a ground plane and spiral antennas that cannot be printed on a plane.

Traditional circularly polarized loop antenna is designed to be used in wireless communication systems with 50Ω input impedance [6–8]. These designs can easily find a 50Ω feeding position on the radiating element and stimulate circularly polarized wave radiation. However, in RFID systems, the tag chip has a capacitive impedance, requiring the antenna to be designed with an inductive impedance to achieve impedance match. Wagih *et al.* [9] and Chen *et al.* [10] discussed the impedance measurement process of UHF RFID conductive fabric tags and the calculation of fabric conductivity. It is worth noting that it is not easy to find a feeding position on the antenna that has a specific inductive input impedance and can excite CP radiation. In [11–14], the authors introduced a certain wide gap in the loop antenna to excite the traveling wave current distribution, resulting in circular polarization. In [15, 16], the authors twisted the loop into a cross shape to form an antenna name cross spiral antenna (CSA). By adjusting the length of the horizontal and vertical arm of the CSA, it can excite the E_θ and E_ϕ components and generating CP waves.

This paper proposes a low-profile circularly polarized loop antenna. The organization of this article is as follows. In the Section I, the design principles of circularly polarized antennas are discussed. This design is incorporate two feeding strips into a square loop with an open gap to disturbs the current distribution on the antenna and excite CP radiation. Next, an inverted U-shaped impedance matching strip is connected in parallel at the feed point, which can compensate for the insufficient input inductance of the antenna, achieve impedance matching with the tag chip. In Section III, simulating the effects of different structural parameters on the circular polarization characteristics and input impedance of tag antenna. Finally, a circularly polarized loop antenna prototype was fabricated and measured. The proposed RFID tag antenna is operable over 2.33–2.55 GHz frequency range.

II. ANTENNA DESIGN

Fig. 1 shows the geometric and detailed dimensions of the direct-feed CP tag antenna with size of $32\text{ mm} \times 32\text{ mm}$. This loop antenna has a compact planar surface area of $32\text{ mm} \times 32\text{ mm}$, and is fabricated on a 0.8 mm FR4 substrate (relative permittivity 4.4 and loss tangent 0.02). The structure includes a square loop, an open gap, two feeding strips and an inverted U-shape matching stub. The proposed CP antenna is designed for an operation frequency (f_0) of 2.45 GHz . It consists of a square loop with side length and width of 32 mm and 1.5 mm , respectively. The total length of the loop antenna is corresponds roughly to 1.5 times wavelength of 2.45 GHz . According to the literature [16], a single square loop antenna cannot excite the CP wave; this study adopts the offset feeding method, and connects two feeding strips with a length of $P_1=20.1\text{ mm}$ and $P_2=4.5\text{ mm}$ to the two points of the outer ring rectangle M and N respectively. An open gap with a length of 0.8 mm is placed at right bottom corner of the square loop. This gap can modify the current

distribution on the loop antenna and excite circular polarization wave.

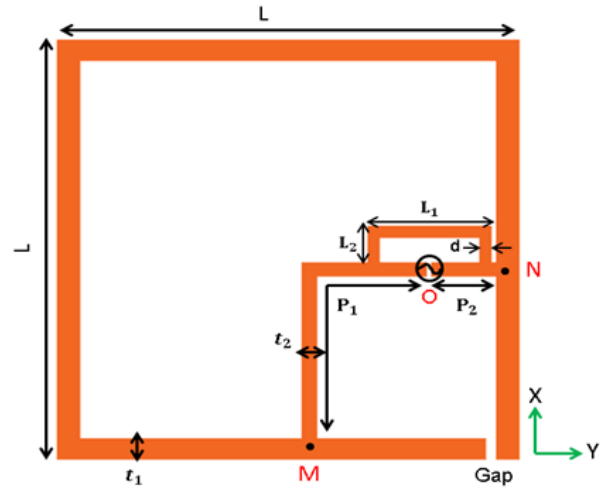


Figure 1. Geometric of the circularly polarized tag antenna. $L = 32$, $t_1 = 1.5$, $P_1 = 20.1$, $P_2 = 4.5$, $t_2 = 1$, $L_1 = 8.54$, $L_2 = 2.88$, $d = 0.77$ (unit: mm).

The tag chip is placed between the two feeding strips, as shown at point O in Fig. 1. To achieve optimal power transfer at 2.45 GHz , the input impedance of the proposed antenna must be conjugately matched with the impedance of the tag chip. To solve this problem, a matching stub with a length of $L_1 = 8.54\text{ mm}$, $L_2 = 2.88\text{ mm}$, and width $d = 0.77\text{ mm}$ is connected to the antenna. This matching stub can be thought of as a shorted transmission line that provides an equivalent inductance. By parallel-connecting it with the loop antenna at the input, matching can be achieved. This antenna is simulated using Ansoft HFSS v.14 full-wave electromagnetic simulator. The correlation of the prepared antenna was measured using an Agilent 8510C vector network analyzer (VNA).

III. RESULTS AND DISCUSSION

First, we will consider the influence of the lengths (L_1 and L_2) of the two feeding strips on the CP characteristics of the antenna. Figs. 2–3 are the polarization axis ratio (AR) and the return loss S_{11} corresponding to varying P_2 when the fixed width of feed point O is 0.4 mm . Figs. 2–3 shows the polarization AR and return loss S_{11} corresponding to different P_2 when the width of the feed point O is fixed at 0.4 mm , respectively. It can be seen from Fig. 2 that the resonant frequency of circular polarization decreases with increasing the P_2 from 4.5 mm to 6 mm . In Fig. 3, it shows that for all different P_2 , the simulated return loss is less than -10 dB (corresponding to $VSWR=2:1$) at 2.45 GHz . Additionally, the impedance bandwidth is about 220 MHz ($2.33 - 2.55\text{ GHz}$) making it suitable for the North American RFID frequency band ($2400 - 2483\text{ MHz}$). Since the operating frequency f_0 is 2.45 GHz , selecting $P_2 = 4.5\text{ mm}$ results in an axial ratio of 1.06 dB and S_{11} of -17.16 dB .

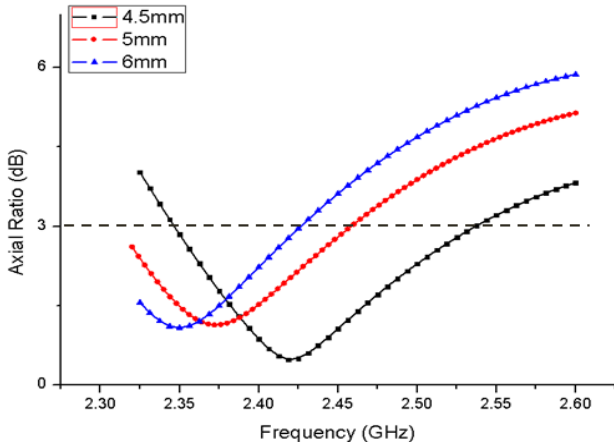


Figure 2. Simulated axis ratio with varying the length P_2 .

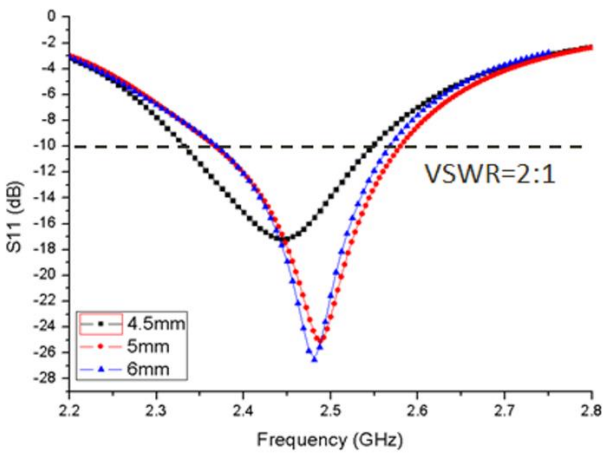
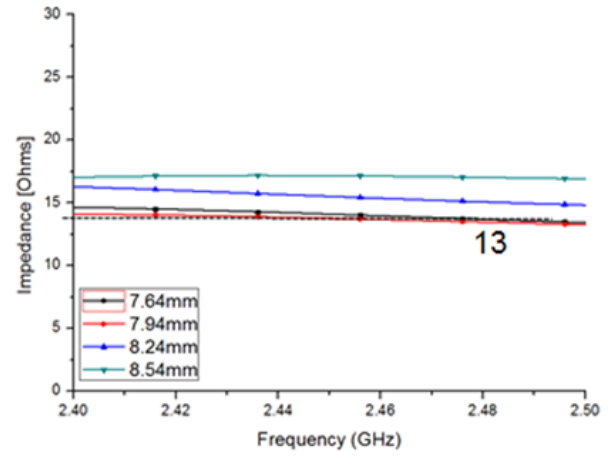
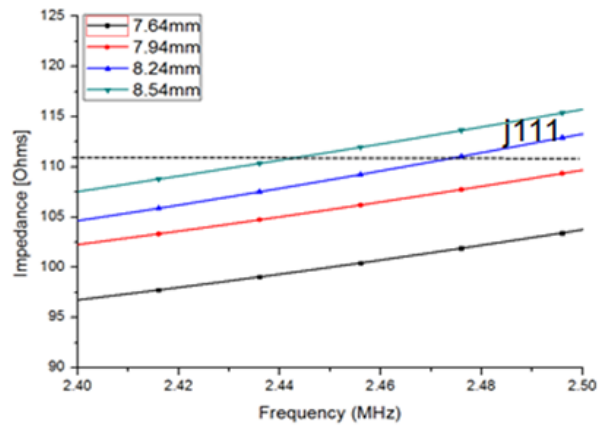


Figure 3. Simulated S_{11} with varying the length P_2 .

The impedance of the chip IC is $13-j111 \Omega$, and the input impedance of the loop antenna without matching stub is $180+j300 \Omega$, which is much larger than the conjugate impedance of the tag chip, resulting in energy transmission loss. To achieve optimal power transfer, the input impedance of the proposed antenna must match $13-j111 \Omega$. Fig. 4 illustrates the simulation of changing L_1 to the antenna input impedance when $L_2 = 28 \text{ mm}$ and $d = 0.77 \text{ mm}$. The imaginary part of the input impedance of loop antenna increases as L_1 increases. In summary, when $L_1 = 8.54$ is selected, the input impedance of the loop antenna is $17+j111 \Omega$ at 2.45 GHz. It is shown that a parallel inverted U-shaped matching stub can increase the reactance of the loop antenna. From Fig. 5, it can be observed that when selecting $L_1 = 8.54 \text{ mm}$, the AR of the loop antenna has the lowest AR at 2.45 GHz. Fig. 5(b) shows that the operating frequency decreases with the increases of L_1 .

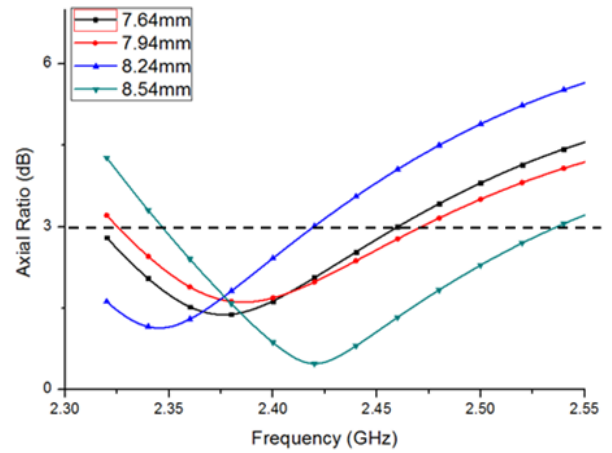


(a)



(b)

Figure 4. Antenna input impedance simulation results:(a) real part, (b) imaginary part. When $L_2 = 28 \text{ mm}$, $d = 0.77 \text{ mm}$ and L_1 is varied.



(a)

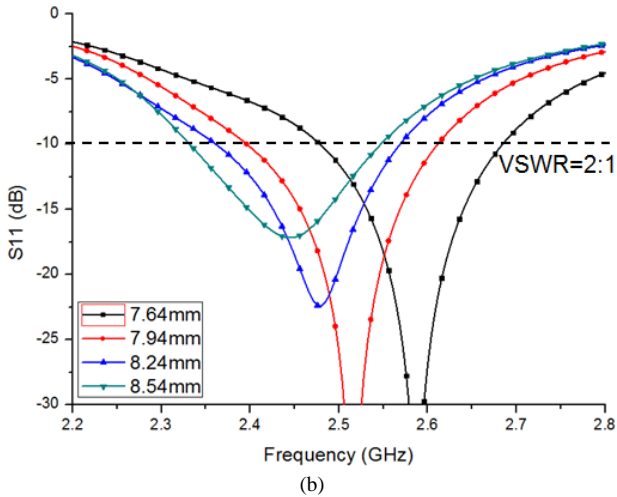


Figure 5. Antenna input impedance simulation results : (a) Polarization axis ratio, (b) S_{11} . When $L_2 = 28$ mm, $d = 0.77$ mm and L_1 is varied.

In the antenna design, the condition for excitation of CP waves is two adjacent modes perpendicular to each other in the polarization direction, with equal electric field intensity and a phase difference of 90 degrees. In this design, an open gap is placed at right bottom of the square loop, and its surface current distribution at 2.45 GHz is shown in Fig. 6. Properly adjusting the position and width of the gap can make the amplitude of the two electric field components of the polarization vertical equal and the phase difference of 90 degrees, it can excite CP waves. Fig. 6 shows the current flow on the surface of the CP tag antenna at 2.45 GHz and 0° , 180° and 270° . It can be seen that when switching from 0° to 270° , the zero point of the surface current will be found to run clockwise from the upper left to the left, which represents the LHCP type. In this case, the LHCP can be from 2.34GHz to 2.53GHz, the axial polarization ratio level at the center frequency (2.45GHz) is 1.06dB, and a broad 3-dB AR bandwidth axial ratio bandwidth is 7.7%.

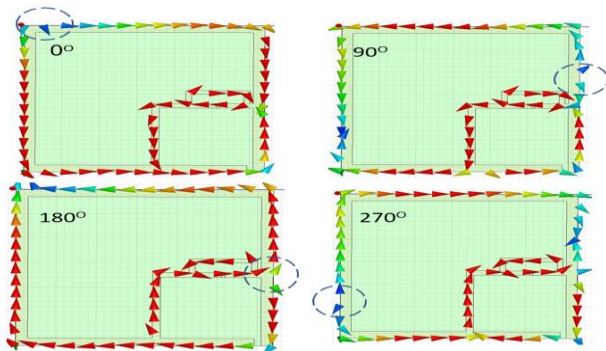


Figure 6. Simulating current flow on the surface of the circularly polarized tag antenna at 2.45 GHz and 0° , 90° , 180° and 270° .

Fig. 7 shows the radiation pattern of the loop antenna in the direction of $\Phi = 0^\circ$ at 2.45GHz. It is well known that the condition for generating circularly polarized waves is the presence of two adjacent modes with perpendicular polarization directions, where the electric field strengths are equal and have a phase difference of 90 degrees. In Fig. 7, at angles of 22.5° , 160° , 230° , and 310° , the GainPhi

value overlaps the GainTheta value, indicating that the amplitude at these points plus the phase difference is 90° , therefore circular polarization can be an excited characteristic.

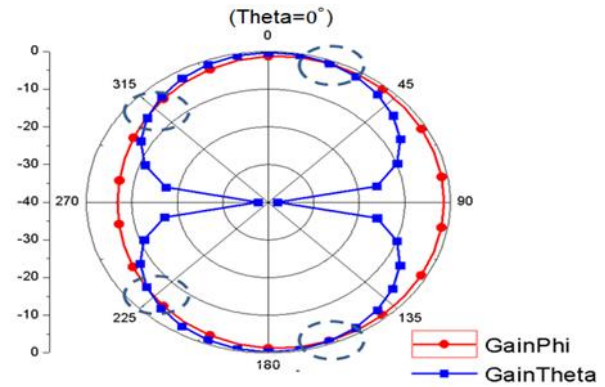


Figure 7. Simulated radiation pattern at 2.45GHz for the proposed antenna.

Fig. 8(a) shows the photograph of the fabricated CP loop antenna. Since the network analyzer has 50Ω system architecture, it is impossible to measure the S_{11} reflection coefficient of the CP loop antenna at the operating frequency of 2.45 GHz with an impedance of $13 + j111 \Omega$. The measured impedance was found to be similar to the simulated results shown in Fig. 8(b). Point A is the ideal conjugate impedance of the tag chip, and its impedance is $13 + j111 \Omega$. The Point B and C show the simulated and measured impedance at 2.45 GHz, respectively. It is found that the measured impedance is similar to the simulated results.

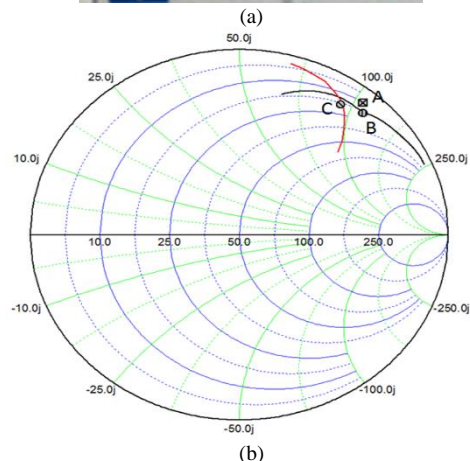


Figure 8 (a). Photograph of the fabricated CP loop antenna, (b) Simulated (black line) and measured (red line) Smith-chart.

To emphasize the importance of miniaturization, a comparison of the proposed antenna with some other 2.45GHz CP RFID tag antennas from [17–19] is presented in Table I in terms of size, reflection loss, and bandwidth. It can be seen that the proposed antenna has the smallest size than the other antennas. Unlike microstrip antennas that typically require a ground plane, the proposed antenna can be produced using printing techniques (e.g., by replacing the substrate with PET), which can lower manufacturing complexity and costs (see Table I).

TABLE I. COMPARISON BETWEEN THE PROPOSED ANTENNA AND OTHER RESEARCH PAPERS

Size (mm ³)	S ₁₁ (dB)	Impedance bandwidths (MHz)	3dB AR bandwidth (MHz)	Ref.
55×55×0.6	-33	100	102	[17]
80×80×8.5	-23.6	640	500	[18]
70×90×0.8	-31	500	180	[19]
32×32×0.8	-17.16	220	190	Proposed antenna

IV. CONCLUSIONS

This paper utilized an offset feeding strips and introduced an open gap in the loop antenna to induce left-hand circular polarization characteristics. The impedance matching between the loop antenna and the chip IC is accomplished by adjusting the inverted U-shaped matching stub. The optimal geometric dimensions of the loop antenna can be obtained through simulation using HFSS software. Following experimentation, measurement, and analysis, the loop antenna and the tag chip achieve impedance matching, the reflection coefficient S_{11} is -17.16 dB at 2.45 GHz, the -10dB impedance bandwidth of the antenna is about 220 MHz (2.33 – 2.55 GHz), and the 3dB AR bandwidth is about 190 MHz (2.34 – 2.53 GHz), the tag antenna designed in this paper has good characteristics at 2.45 GHz, and is suitable for microwave RFID applications.

By utilizing the design method proposed in this paper and replacing the FR4 substrate with PET, the RFID tag antenna can be manufactured using printing technology. Which will have the advantages of low profile, low cost, and flexibility. This will result in an antenna with a low profile, low cost, and flexibility, making it suitable for attachment to textiles and curved objects.

CONFLICT OF INTEREST

The authors declare no conflict of interest.

AUTHOR CONTRIBUTIONS

Conceptualization, S.-T W.; methodology, C.-L.P.; validation, P.-C.C.; formal analysis, Y.-F.C.; investigation, Y.-F.C.; data curation, Y.-F.C.; writing—original draft preparation, C.-L.P., writing—review and editing, C.-L.P.; supervision, P.-C.C.; project administration, C.-L.P.;

funding acquisition, S.-T W. All authors have read and agreed to the published version of the manuscript.

REFERENCES

- [1] K. Finkenzeller, *RFID Handbook: Fundamentals and Applications in Contactless Smart Cards and Identification*, John Wiley & Sons, Munich, 2003.
- [2] S. Kumar *et al.* “Dual circularly polarized planar four-port MIMO antenna with wide axial-ratio bandwidth,” *Sensors*, vol. 20, p. 5610, 2020.
- [3] S. J. Yoon and J. H. Choi, “A ka-band circular polarized waveguide slot antenna with a cross iris,” *Appl. Sci.*, vol. 10, p. 6994, 2020.
- [4] C. Cho, I. Park, and H. Choo, “Design of a circularly polarized tag antenna for increased reading range,” *IEEE Trans. Antennas Propag.*, vol. 57, no. 10, pp. 3418–3422, 2009.
- [5] D. D. Deavours, “A circularly polarized planar antenna modified for passive UHF RFID,” in *Proc. 2009 IEEE International Conference on RFID*, pp. 265–269, 2009.
- [6] H. Morishita and K. Hirasawa, “Wideband circularly-polarized loop antenna,” in *Proc. IEEE Antennas Propag. Soc. Int. Symp.*, vol. 2, pp. 1286–1289, 1994.
- [7] K. Hirose, T. Haraga, and H. Nakano, “A momople-fed circularly polarized loop antenna,” *IEEE Antennas Propag. Soc. Int. Symp. Dig.*, pp. 1–4, 2010.
- [8] F. K. Byondi and Y. Chung, “UHF RFID conductive fabric tag design optimization,” *Sensors*, vol. 21, p. 5380, 2021.
- [9] M. Wagih *et al.* “Reliable uhf long-range textile-integrated RFID tag based on a compact flexible antenna filament,” *Sensors*, vol. 20, p. 3435, 2020.
- [10] H. D. Chen, C. H. Tsai, C. Y. D. Sim, and C. Y. Kuo, “Circularly polarized loop tag antenna for long reading range RFID applications,” *IEEE Antennas and Wireless Propagation Letters*, vol. 12, pp. 1460–1463, 2013.
- [11] C. H. Tsai, H. D. Chen, and C. Y. D. Sim, “High-gain circularly-polarized loop tag antenna for long reading distance RFID application,” *Microwave. Opt. Technol. Lett.*, vol. 56, no. 10, pp. 2335–2341, Oct. 2014.
- [12] H. Chen, C. Sim, C. Tsai, and C. Kuo, “Compact circularly polarized meandered-loop antenna for UHF-Band RFID tag,” *IEEE Antennas Wireless Propagation. Letter*, vol. 15, pp. 1602–1605, 2016.
- [13] J. H. Lu and B. S. Chang, “Planar compact square-ring tag antenna with circular polarization for UHF RFID applications,” *IEEE Transactions on Antennas and Propagation*, vol. 65, no. 2, pp. 432–441, 2017.
- [14] M. Matsunaga, “A simple circular polarized loop antenna,” in *Proc. IEEE Antennas Propagation. Soc. Int. Symp.*, 2014, pp. 575–576.
- [15] M. Matsunaga, “A linearly and circularly polarized double-band cross spiral antenna,” *IEICE Trans. Commun.*, vol. E99-B, no. 2, pp. 430–438, 2016.
- [16] H. Morishita and K. Hirasawa, “Wideband circularly-polarized loop antenna,” in *Proc. IEEE Antennas Propag. Soc. Int. Symp.*, vol. 2, pp. 1286–1289, 1994.
- [17] G. Chaouki, G. Said, A. Olf, and G. Ali, “An electrical model to L-slot square patch antenna,” in *Proc. 2017 International Conference on Internet of Things, Embedded Systems and Communications (IINTEC)*, 2017.
- [18] L. L. Wan, S. H. Chen, and N. Zhou, “Broadband circularly polarized antenna design and simulation for 5G IoT applications,” in *Proc. 2021 International Conference on Electronic Information Technology and Smart Agriculture (ICEITSA)*, 2021.
- [19] A. Azarbar, M. Mashhadi, and J. Ghalibafan. “A novel circularly polarized dual-band slot antenna for RFID applications,” in *Proc. 2011 IEEE GCC Conference and Exhibition (GCC)*, 2011.

Copyright © 2023 by the authors. This is an open access article distributed under the Creative Commons Attribution License ([CC BY-NC-ND 4.0](https://creativecommons.org/licenses/by-nc-nd/4.0/)), which permits use, distribution and reproduction in any medium, provided that the article is properly cited, the use is non-commercial and no modifications or adaptations are made.